International Journal of Progressive Sciences and Technologies (IJPSAT)
ISSN: 2509-0119.

http://ijpsat.ijsht-journals.org
Vol. 30 No. 1 December 2021, pp.01-16

# Geophysical Investigation Of Possible Gold Mineralization Potential Zones Using A Combined Airborne Magnetic Data Of Lower Sokoto Basin And ITS Environs, Northwestern Nigeria

M. M. Lawal[1], K. A. Salako[2], M Abbas[3], T. Adewumi[4], A. I. Augie[5], M. Khita[6]

[1, 3]Department of Physics, Kebbi State University of Science and Technology, Aliero.
[2]Department of Geophysics Federal University, Minna.
[4]Department of Physics Federal University Lafiya, Nasarawa.
[5] Department of Geophysics Federal, University Birnin Kebbi, Kalgo.

[6]Department of Geology Usmanu Danfodiyo University Sokoto-Nigeria



**Abstract – Delineation of possible gold mineralization within the lower Sokoto basin from analyses and interpretation of airborne magnetic and radiometric datasets has been successfully carried out in this present study. In achieving this, some enhancing filters such as; first and second vertical derivatives, horizontal derivatives, and analytic signal and center for exploration targeting were applied on the total magnetic field of the study area to delineate near-surface structures that might host the gold deposit in the study area. Also Source Parameter Imaging was used to estimate the depth of the buried structures. K/eTh ratio was performed to identify the hydrothermal alterations zones for gold mineralization within the study area. The first and second VD, the horizontal derivatives and the CET revealed major structures like trending NE-SW, NNE-SSW and NW-SE. The AS revealed the boundary demarcation between the crystalline rocks and the sedimentary rocks. The crystalline rocks occupy the eastern and western part of the study area with the sedimentary rocks in between lying NW-SE. The SPI result reveals a shallow depth of 68.21- 101.60 meters. The radiometric data enhancement (K/eTh) helped in identifying areas of hydrothermal altered zones; this could be observed at the NE and some portions along the SW zone of the study area which are favorable alteration environments for a variety of ore deposits. The areas affected by hydrothermal alteration are considered mineral potential zones and may be promising sites for gold mineralization.**

**Keywords – Aeromagnetic; Aeroradiometric; Hydrothermal Alteration: Center for Exploration Targeting (CET); Lineaments.**

## I. Introduction

There is no doubt that the major revenue generation that drives the Nigeria's economy is derived from the export and domestic sale of oil and gas (crude oil) for foreign exchange. With the rise and fall in the price of oil in the world oil market, there is a need to look into other viable sources through which revenue could be generate to sustain the economy such as exploration of economic and solid minerals.

With the recent priority attention given to the diversification of the Nigerian economy, the development of the solid mineral sector has become very important. This is due to the realization of the crucial role the solid mineral sector can play in revamping the nation's economy. The use of gold as an ornament and as money makes it a precious metal with an accompanying rush for exploration and exploitation worldwide. Magnetic and radiometric method have proved useful in the direct detection of mineralization (e.g. iron ore deposits and heavy mineral sands) for the location of favorable host rocks such as carbonites, kimberlite, porphyritic intrusion, defective and hydrothermal alteration, which are strong indicator for gold mineralization zones and for mapping geologic features of prospective areas (Roux, 1970; Macnae, 1979; Hoover *et al.,* 1992, Keating, 1995; Biegert *et al.,* 1998; Power *et al.,* 2004; Amigun *et al.,* 2012). Minerals occur in three main metallogenic provinces viz: the Precambrian Basement Complex, the Jurassic Younger Granites and Cretaceous-Tertiary sedimentary basins (Akande and Kinnaird, 1992). In Nigeria, several authors have shown that there are many areas of the occurrence of gold in the Nigerian Schist Belts, especially in the western part of the country (Adekeye *et al.,* 2015).

The focus on how to locate minerals deposits in the country has taken a Centre stage. Gold deposit is by far the most important target in the Basement Complex of Nigeria and contains world class potential gold reserves. Structural and hydrothermal alterations, which are critically important in controlling gold mineralization throughout the Schist Belts can usually, be observed directly in the magnetic and radiometric patterns (Armstrong and Rodeghiero, 2006).

The gold deposits in placers and primary veins commonly occur in alluvial stream sediments and in quartz veins respectively within several lithologies of the supracrustal belts (Adekeye *et al.,* 2015). The primary gold mineralization found in supracrustal and basement are commonly associated with veins, stringers, reefs and similar bodies like quartz, quartz-feldspartic, Amphibole Schist, porphyritic granite and quartz-tourmaline rocks.

Lithologic units, lithologic boundaries, veins, fractures and mineral accumulations are more accurately identified and delineated using the combination of surface geological mapping, geophysical data, and geochemical data on subsurface samples. Aeromagnetic geophysical prospecting employs high magnetic susceptibility contrast between basement rocks to identify and map different lithologic units, geological structures and mineral accumulations within basement terrains (Kearey *et al.,* 2002; Osinowo *et al.,* 2014).

## II. GEOLOGY SETTING AND LOCATION OF THE STUDY AREA

The area under consideration covers an approximate area of 12,100 sq.km, and lies between latitude $10^0$ 00 to $11^0$ 00 N and longitude $4^0$ 00 to $5^0$ 00 E (Figure 1). The study area covers extensively the lower Sokoto Basin, upper Bida Basin and the older granites of Basements Complex. The Basement Complex rocks are of the Precambrian age (Obaje, 2009) and comprise of Migmatite–Gneiss Complex, Older Granite and the schist. The sedimentary rocks belong to the Sokoto/Lullemenden Basin and of the Taloka Formation, comprising of sandstone, siltstone, and claystone. This Basin is believed to have been formed by tectonic epirogenic movement or stretching and rifting of the tectonically stable crust during the Paleozoic (Ajibade *et al.,* 1987). All the rocks in the area belong either to the Upper Cretaceous or to the Precambrian as shown in figure (2). The geology of the study area have been described in detail by various works of (McCurry, 1978; Ajibade, 1976; Wright, 1976). The dominant tectonic fabric in the region is a steeply dipping N-S phyletic to salty cleavage, which is generally axial planer to isoclinal folds (Garba, 1994). According Garba (1994), the gold deposit in the area comprises epigenetic vain-type mineralization within a late tectonic brittle fault zone that transverses the hornfelsed contact zone of the granodiorite intrusion.

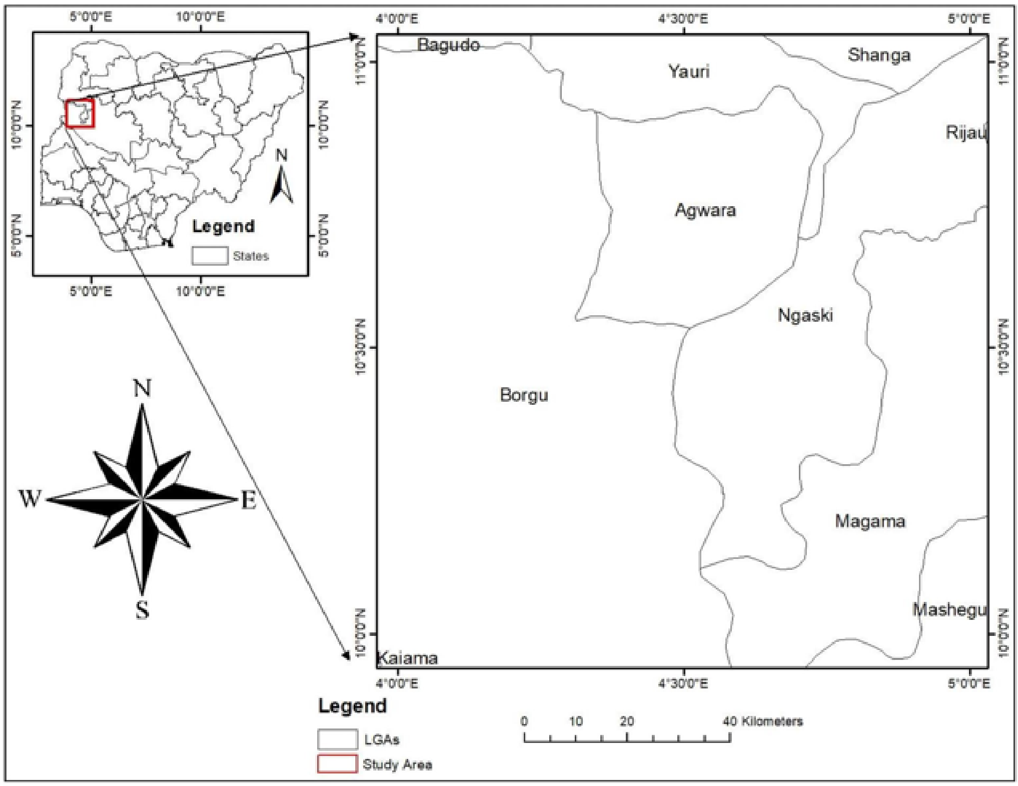


**Figure 1.1: Geological Map of Nigeria showing the stody area in red outline**

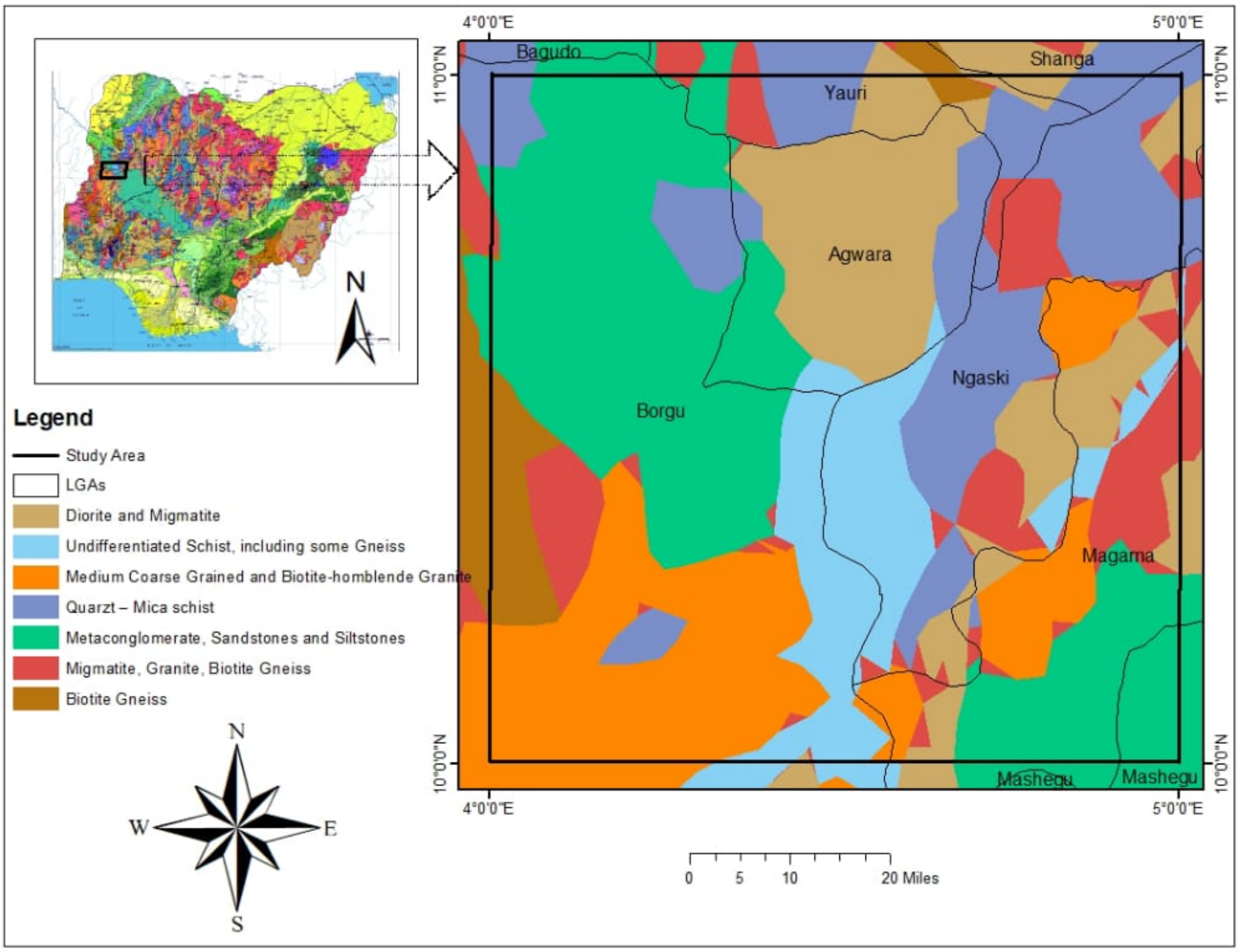


**Figure 1.2: Geologic Formation of The Study Area ( Global Map Softwire)**

## III. Materials and Methods

**Data Acquisition**

For the purpose of this work four high-resolution aeromagnetic and aeroradiometric data covering the study area respectively were obtained from Nigerian Geological Survey Agency (NGSA). The data were acquired along a series of NE-SW flight lines with a spacing of 200 m and an average flight elevation of about 80 m while tie lines occur at about 500 m interval. The geomagnetic gradient was removed from the data using the International Geomagnetic Reference Field (IGRF), the data were made available in the form of grids on a scale of 1:100,000. These data were processed and merged together into a common dataset

**Methodology**

The first step taken was assembling and knitting of the airborne magnetic and radiometric datasets in separate sheets of 55 x 55 km2 to form the composite maps of the total magnetic field and the concentration maps of the radioelements (K, eTh and eU) respectively using Oasis Montaj v8.4. thereafter, some enhancing techniques such as; vertical derivatives, horizontal derivatives, analytic signal, center for exploration targeting (CET) were applied to the TMI to delineate near surface structures that might host gold mineralization within the study area. Also Source parameter imaging (SPI) was employed to estimate the depth of the structures.

**Vertical Derivatives**

The vertical derivative is commonly applied to total magnetic field data to enhance the shallow geological sources. The enhancement sharpens the edges of the anomalies over bodies and tends to reduce anomaly complexity allowing clearer imaging of a causing structure (Adewumi & Salako, 2018). The second vertical derivatives are also used to delineate geological boundaries between rocks with contrasting physical properties such as magnetic susceptibility. The contoured second vertical derivative outlines the bodies causing the magnetic anomalies.

The equation for the computation of vertical derivatives ($\frac{\partial^n T}{\partial z^n}$) of the magnetic field data T as shown by Collins (2005) and Hinze *et al.,* (2013) is;

$$F\,\frac{\partial^n T}{\partial z^n} = K^n\, F(T) \tag{1}$$

**Analytic signal**

The analytic signal technique is based on the use of the first derivative of magnetic anomalies to estimate source characteristics and to locate positions of geologic boundaries such as contacts and faults. The amplitude of Analytic Signal (AS) is defined as the square root of the squared sum of the vertical and the two horizontal first derivatives of magnetic field anomaly T and is given by Roest *et al.,* (1992):

$$|A(x,y,z)| = \sqrt{\left(\frac{\partial \mathrm{M}}{\partial \mathrm{x}}\right)^2 + \left(\frac{\partial \mathrm{M}}{\partial \mathrm{y}}\right)^2 + \left(\frac{\partial \mathrm{M}}{\partial \mathrm{z}}\right)^2} \tag{2}$$

where; $A\,(x, y) =$ amplitude of the analytic signal at $(x, y)$,

$M =$ observed magnetic field at $(x, y)$.

**Source Parameter Imaging**

The Source Parameter Imaging TM (SPI) function is a fast, simple, and capable method for computing the depth of magnetic sources. Its accuracy has been demonstrated to be +/- 20% in tests on real data sets with drill hole control. This accuracy is analogous to that of Euler deconvolution, however SPI has the advantage of delivering a more complete set of coherent solution points and it is easier to use (Salako, 2014). One merit of the SPI technique is that the depth can be visualised in a raster format and the true thickness can be determined for each anomaly.

**Center for Exploration Targeting (CET)**

The Centre for Exploration Targeting (CET) grid Analysis and CET Porphyry Analysis algorithm developed and incorporated as extension into the Geosoft Oasis Montaj software (Geosoft, 2014) were used in this study for lineament. Structural and porphyry mineral deposit mapping. CET Grid Analysis is a suite of algorithms which provides functionalities for enhancement, lineament detection and structural complexity analysis of potential field data Core *et al.* (2009). This technique automatically delineates lineaments and identify promising areas of ore deposits via outlining regions of convergence and also divergence of structural elements using several statistical steps that include texture analysis, lineation delineation and Vectorization and complexity analysis to generate contact occurrence density map (Kovesi, 1991; Lam *et al.,* 1992; Kovesi, 1997; Holden *et al*., 2008; Holden *et al.,* 2010).

**Aeroradiometric data**

The data is to register and understand radiometric signatures associated with the host rocks that are important to mineralization, enhancing techniques such as composite image, ratio maps as well as potassium (K%), thorium (eTh) and uranium (eU) maps were used. Some gold deposits show increases in K and decrease Th, which suggest that Th was mobilized in hydrothermally altered systems *Silva et al., (2003)*, also producing K/eTh ratio map help to map hydrothermally altered zones, since a reduction in eTh and a rise in K is an indicator of alteration environments in an ore deposit (Ostrovskiy, 1975) many studies were conducted for identifying alteration zones (e.g. Irvine and Smith, 1990; Feebrey *et al.,* 1998; Morrell *et al.,* 2011; Wemegah *et al.,* 2015).

## IV. Results and Discussion

In the present work, aeromagnetic and aeroradiometric data of a part of the lower Sokoto basin, Upper Bida Basin and a portion of Basement Complex were analyzed and interpreted qualitatively and quantitatively with the aim of delineating gold deposits within the study area.

**Aeromagnetic Results**

The total magnetic intensity (TMI) map of the study area (Fig. 3) revealed variation in magnetic intensity which may be attributed to several effect or factors such as lithology difference, variation in depth of magnetic source, degree of strike and microstructures which form major control of geophysical methods of investigation (Dentith and Mudge, 2014). The magnetic intensity of the study area ranging from -63.69 to 123.32 nT.

The first vertical derivatives (Fig. 4a) the magnetic signal ranges –3.895 nT/n to 3.738 nT/m and the structural trend observed in the NE-SW and the intermediate signals trend NW direction of the study area. The 2VD of total magnetic intensity map (Fig. 4b) represent the point of inflexion on the normal anomaly curve which approximates the location of edges of causative bodies, provided they have vertical sides and are shallow (Chukwuka, 2016).

The second vertical derivative magnetic signals values range from -0.040 nT/m to 0.037 nT/m while the positive and negative anomalies often match surfaces of mafic and felsic rocks respectively (Gupta and Ramani,1982; Opara *et al.,* 2014; 2015). The positive features may be attributed with mafic rocks (rocks with high concentration of magnesium, iron and other minerals) and the negative features may be attributed felsic rocks (acidic) rocks with high concentration of feldspar and silicon and other minerals like aluminum, quartz, muscovite, potassium-rich plagioclase and orthoclase, the two results of first and second vertical derivatives agreed with each other.

Analytical Signal helps in delineating the area into regions of outcrop, intermediate structures and basement under the influence of thick sedimentation (Taiwo & Salako 2018). Three major structures can easily be observed on the map (fig. 5), the area whose has high amplitude, intermediate and low amplitude response and the area with high response are predominantly basement complex while area with low are of sedimentary basement complex.

Center for exploration target analysis (CET) The method was applied to classify the embedded linear structures within the aeromagnetic data, through consecutive map by-product forms Include standard deviation calculating magnetic shifts, then Phase symmetry to distinguish continuous lateral lines. Henceforth the Produced lineaments improved by noise and sound reduction Amplitude-thresholding signals (fig. 6)

It should be noted that the lineaments shown on the CET lineament analysis map (fig. 6) show that the basement rocks overrunning the NE-SW part of the study area and are highly deformed at the central part which covered by sedimentary basin. The orientation can also see trending NNE-SSW direction within the basement complex.

CET porphyry analysis, Detection of porphyry features has been conducted in the present study in four successive steps, including the first circular feature detection. Second, the amplitude contrast transforms the boundary tracing overlaid on the aeromagnetic map of the study area. Finally a geologic contact map that depicts porphyry features was generated (fig. 7). Most of these dike-like features are more abundant above Granite, Migmatite gneiss, undifferentiated schist, Diorite, Quartzites, Porphyritic Gneiss and Amphibole schist as show in (fig. 2).

It was observed that these features are in coincidence with the structural complexity of lineament and geologic contact maps Obtainable from both CET grid and porphyry analysis. It is also recognized that these features are located along the NE-SW trend, which represents the preferred orientation for ore deposition and found to have a high probability of more ore deposition in the study area and Mineral occurrences have indeed been found to be, in most cases, above or close to these porphyry characteristics and needs only fellow up in the field to determine its full potential.

The evident structural trends observed in 1VD, 2VD, Lineaments and Geological Contact maps have been agreed upon and, furthermore, this information will be more valuable when integrated with the radiometric dataset used to recognize potential hydrothermal alteration zones within the study area.

The map of the Source Imaging Parameter (SPI) (Fig. 8) shown various colors that indicate different depth values of magnetic source bodies from – 68.21 m to – 229.62 m for shallow magnetic sources or near-surface intrusive magnetic sources while – 224.19 m to – 2979.17 m it's for deep magnetic sources (including deep-seated faults and crystalline basement topography). The values of the depth are Marked by the legends of the blue, yellow, pink and red colors and the negative sign is indicating depth to magnetic anomalous. The white areas / potion of (fig. 8) are the areas where the derivative used to estimate the local wave number is so small that the SPI is so small the structural index cannot be measured reliably.

**Aeroradiometric Results**

The variations in the mineral content of surface geology can be better explained by the use of radiometric survey data, which is also useful in mapping lateral lithologies. Aeroradiometric distribution of potassium data (K), equivalent uranium (eU) and thorium equivalents (eTh) on the research area is described in the (fig. 9a, b and c) respectively. The measured concentration of potassium map (%) range - 0.44 to 7.84 % which correspond to (-137.72 Bq/kg to 2463.31 Bq/kg) in (fig.9a) and it shows different degree of potassium percentage and reflects different lithological structure. Potassium emission is primarily caused by potash feldspars, which are mostly prevalent in felsic igneous rocks (e.g. granite) and are weak in mafic rocks (e.g. basalts and andesite) and the high signature of K % was observed NE and SW direction whilst the very low % is at the central part of the study area.

The measured concentration of equivalent Thorium map (fig. 9b) ranges -5.48 ppm to 135.39 ppm which corresponds to –22.249 Bq/kg to 549.683 Bq/kg for Thorium radiation. The high concentration is trending N-SE, and SW direction, the low values is at the central part whilst moderate value is trending NW of the study area.

The equivalent Uranium concentration (eU) map (fig. 9c) shows different range of eU concentrations of -1.74 ppm to 17.51 ppm corresponds to -21.501 Bq/kg to 216.249 Bq/kg for Uranium radiation and the high signature was observed in NNE and scarred in SW-NW direction whilst the low signature is trending at the central part of the study area.

Generally, the zones of high natural radionuclide of all the nuclear elements are in Northeast and Southern part while the low zone of radioelements signature is at central part of the study area and the high concentration zones indicate the region associated with the crystalline basement and the presence of intrusive formation. The low concentrations of K, eTh and eU at the central part of the region were such that low radioactivity was not more than 30 % of the total field, suggesting the presence of carbonate, silicate formation and quaternary sediments.

However, the relationship between U and Th is linear, indicating that U and Th complement each other. The high concentrations of U and Th are characteristic of the widespread intrusive rocks (granite, syenite) in the studied region as well as in other parts of Nigeria (Adepelumi & Falade 2017).

The ratio map of K and Th (Fig. 10) indicates a strong concentration of K (red color) and this indicates a low concentration of Th. Decrease in Th and increase in K incidence as seen along the defective NE and some potions along the SW zone of the study area and are favorable alteration environment for variety of ore deposits (Ostrovskiy, 1975). The ratio map (Fig. 10) depicts this region with high K (red color) and low Th. However, depending on the fact that the ratio between potassium and thorium is rather constant in most rocks, typically varying from 0.17 to 0.2 (K/Th in%/ppm, Hoover et al. 1992). Rocks with K/eTh ratios remarkably outside of this range have been named potassium or thorium specialized (Portnov, 1987) Some potential gold mineralization zones display increases in K and Th, such as NE and SW along lithological contact varying 0.18 to 0.41 region. The K / eTh ratio map (Fig. 10) shows that the areas affected by the hydrothermal process are colored (red pink) and have a high value in the range 0.18 to 0.41 K / eTh ratio (Fig. 10) and these areas is associated with crystalize basement complex and is the areas associated with low magnetic intensity as shown in total magnetic intensity map

The ternary image (Figure 11) comprises of colors produced from the relative intensities of the three components and represents subtle variations in the ratios of the three bands with K assigned to red, U to blue and Th to green. The composite picture provides clear spatial similarities with the recognized geological units and the most prominent features of the K, Th and U images. In some degree, the radiometric responses in the ternary map correspond to the surface geological map of the study area (Fig. 2). High amounts of radioactive elements U, Th and K are seen in black colors with a magenta light corresponding to high levels of potassium with higher levels of uranium and thorium.

Those with a low K content but a high U and Th content are characterized by a green color and the yellow colors are characterized by high potassium and low uranium thorium. In addition, the blue color refers to high uranium regions with low potassium and thorium content.

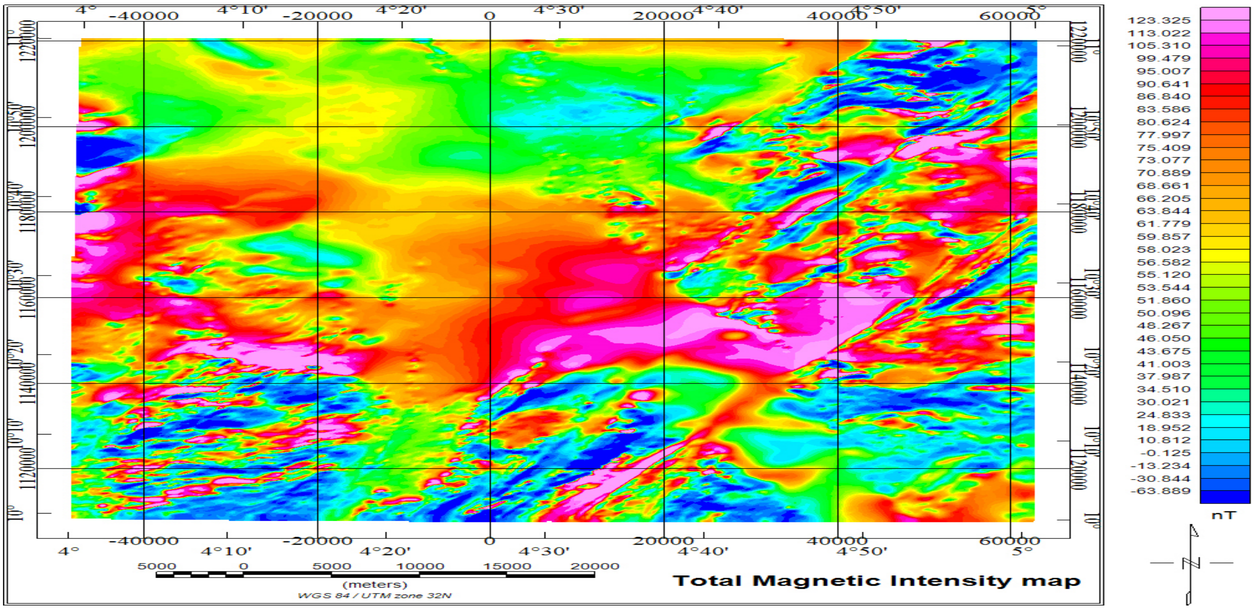


**Fig. 3 Total Magnetic Intensity Map**

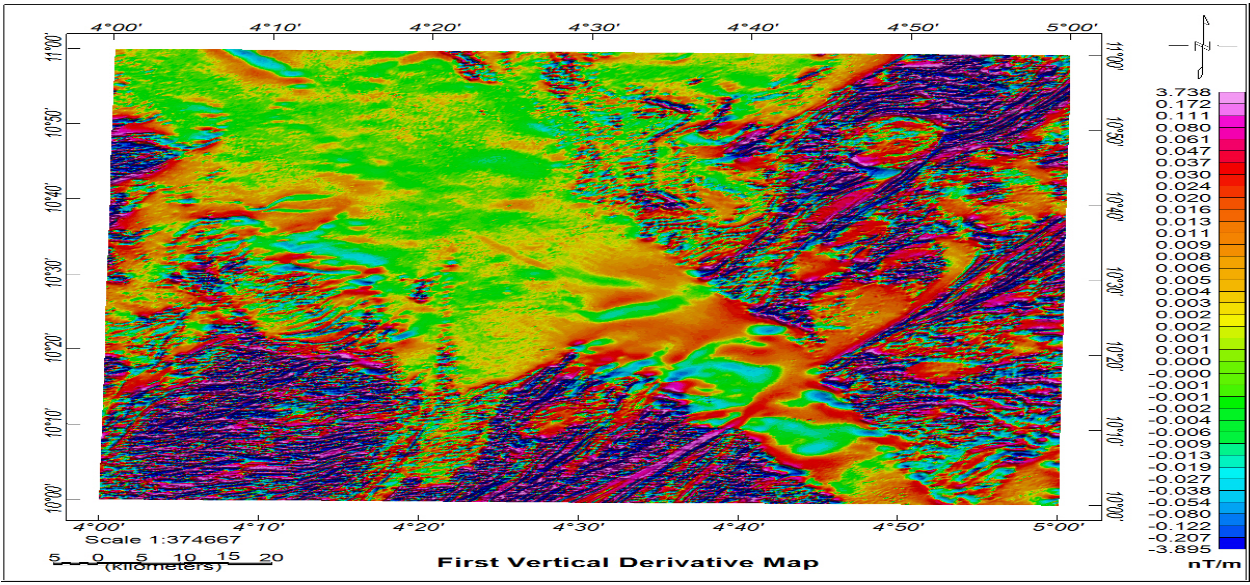


**Fig. 4a First Vertical Derivatives Map**

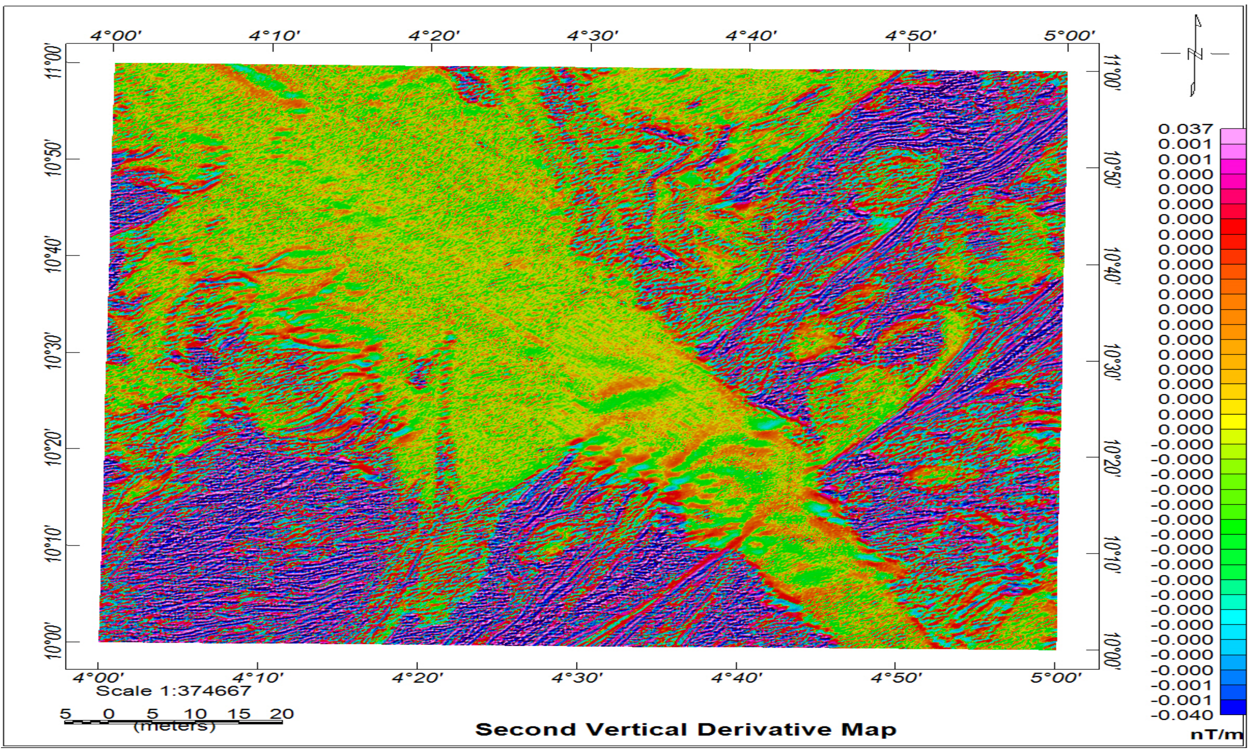

Fig. 4b Second Vertical Derivative Map

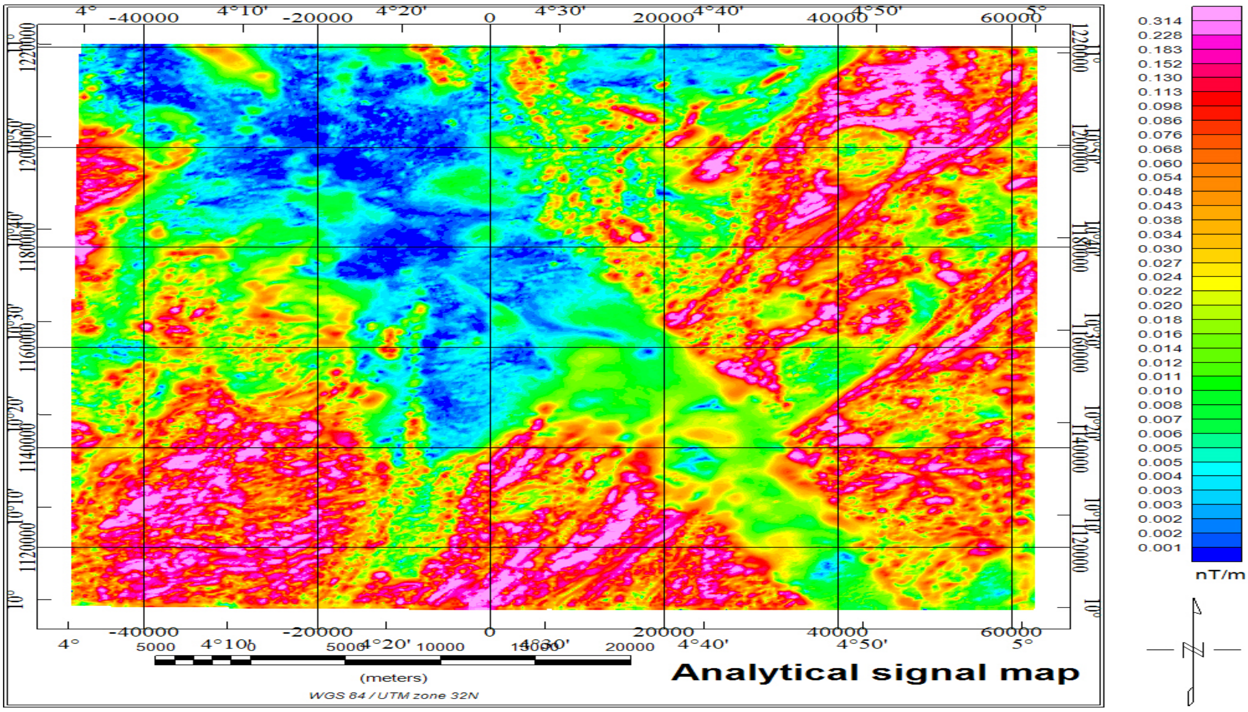

Fig. 5 Analytical Signal Map (AS)

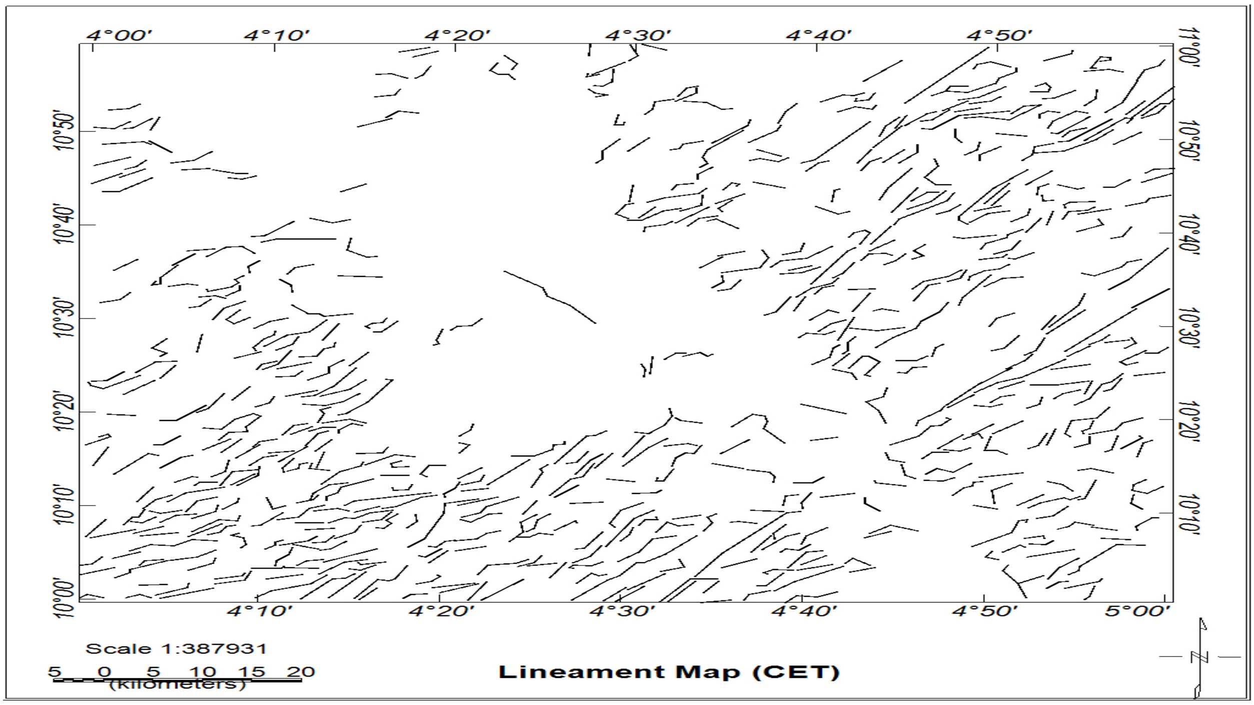


**Fig. 6 CET lineament Analysis Map**

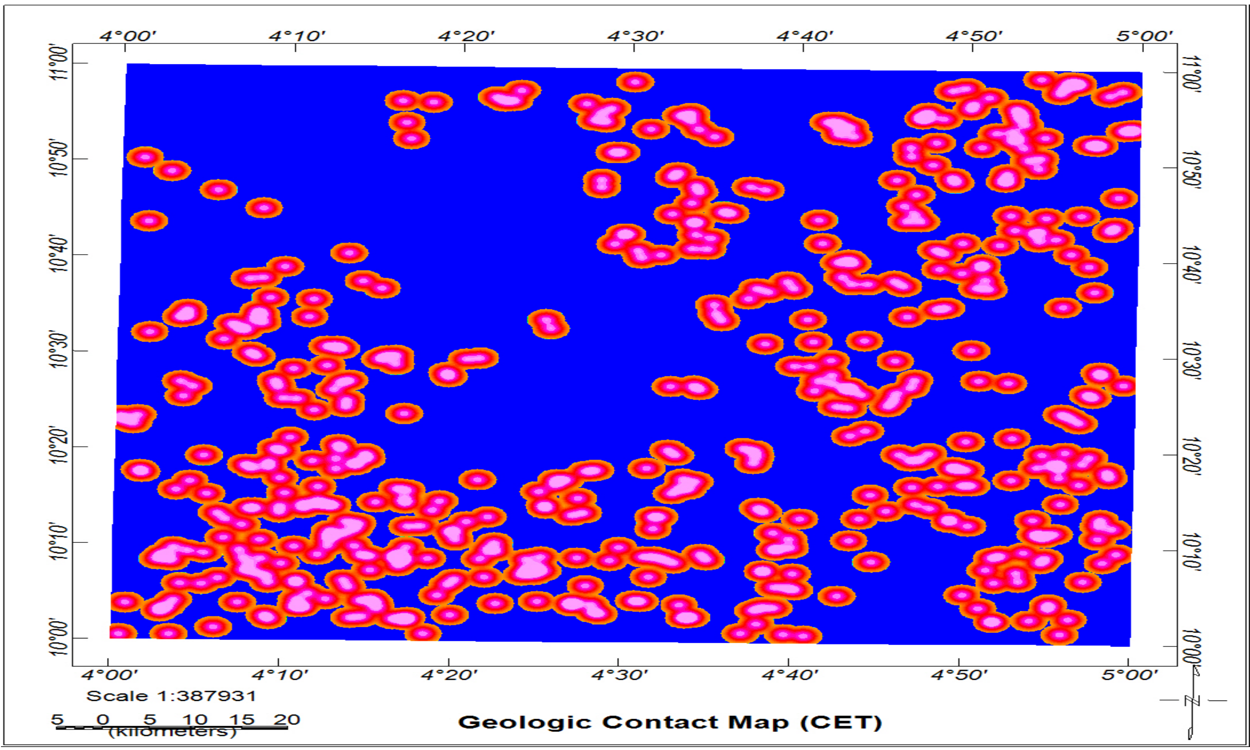


**Fig.7 porphyry analysis Map (CET)**

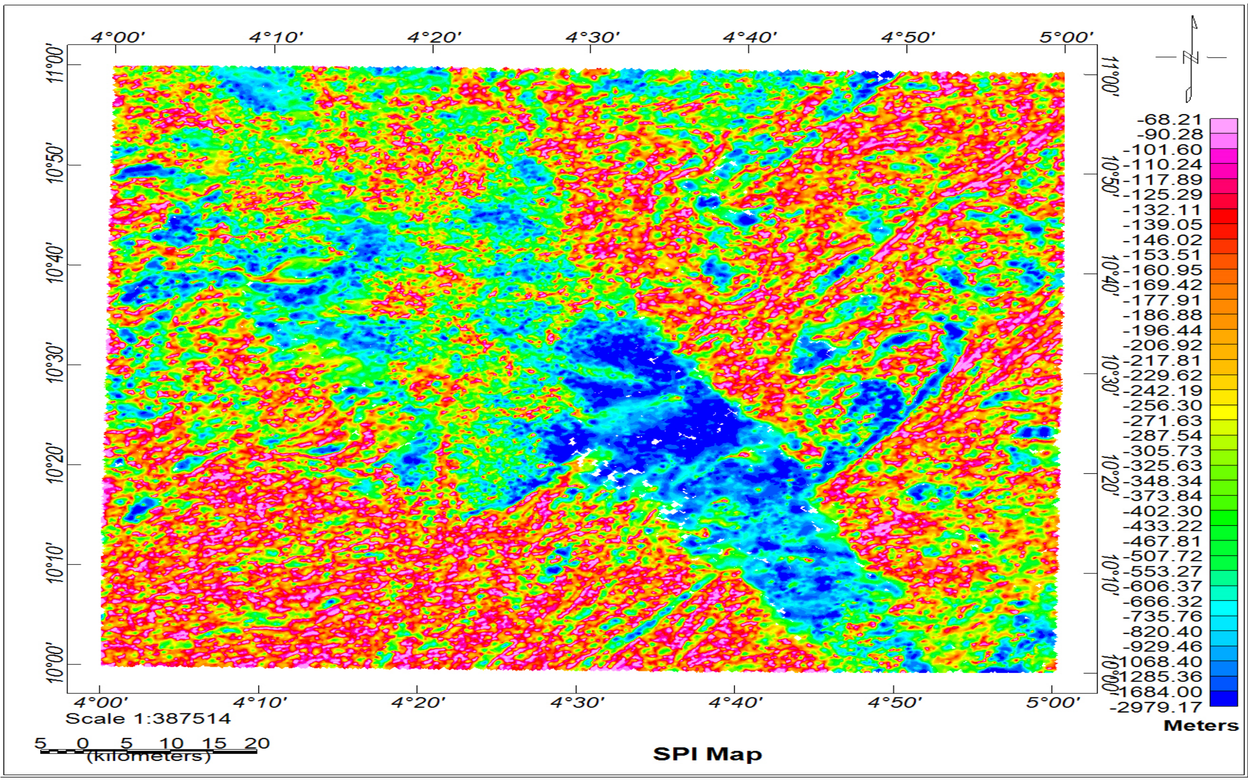


**Fig. 8 Source Parameter Imagine Map (SPI)**

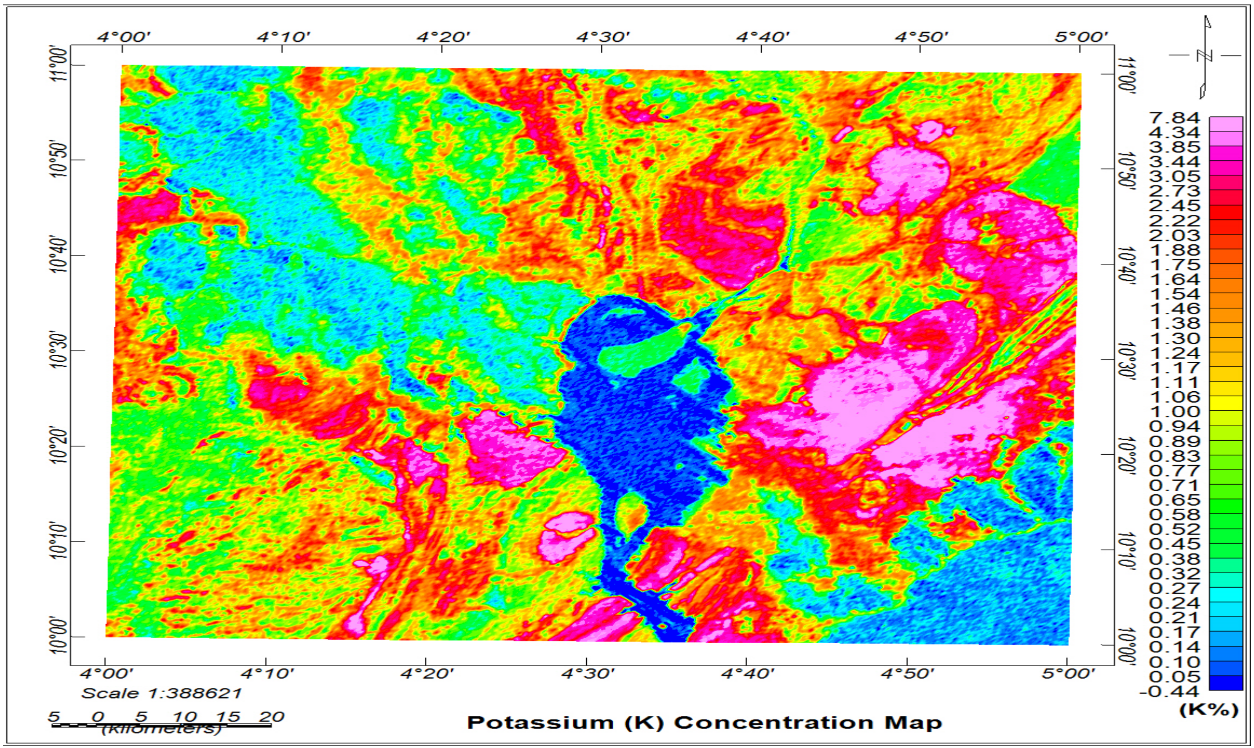


**Fig. 9a Potassium (K %) Concentration Map**

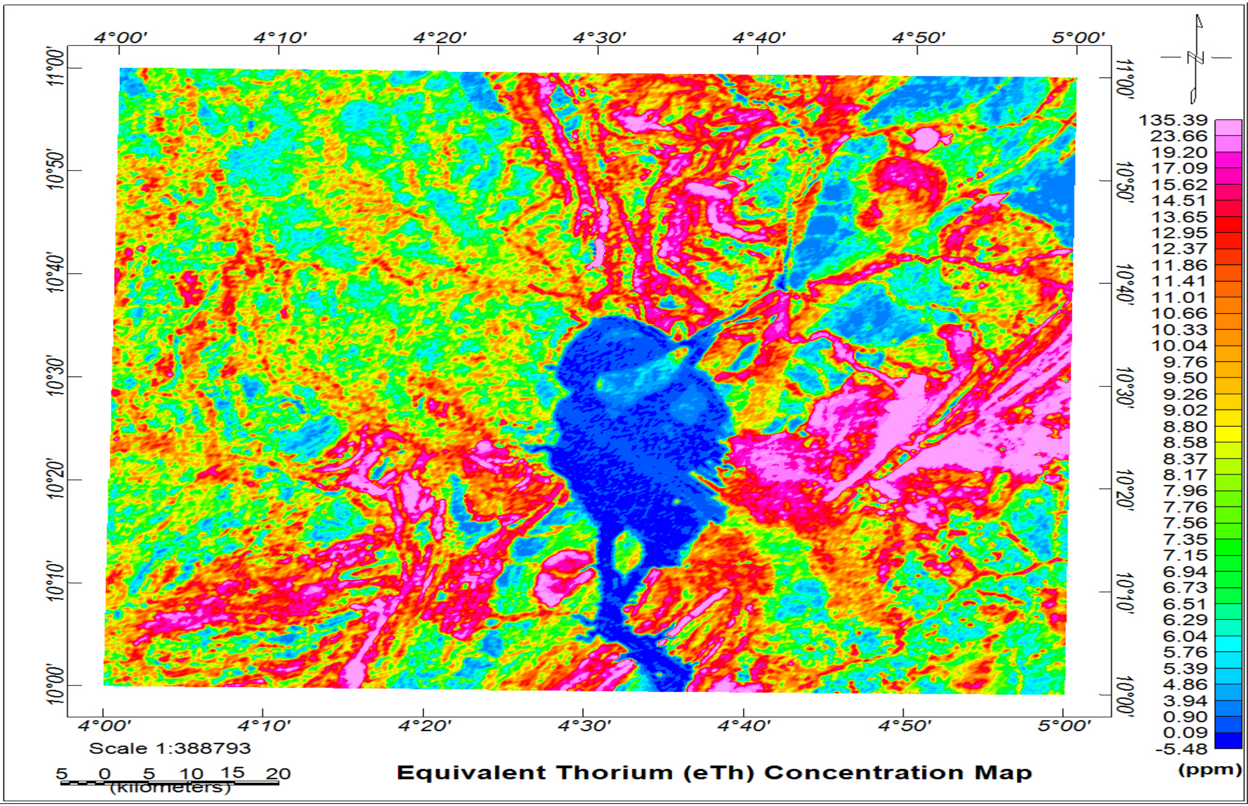


**Fig. 9b Equivalent Thorium (eTh ppm) Concentration Map**

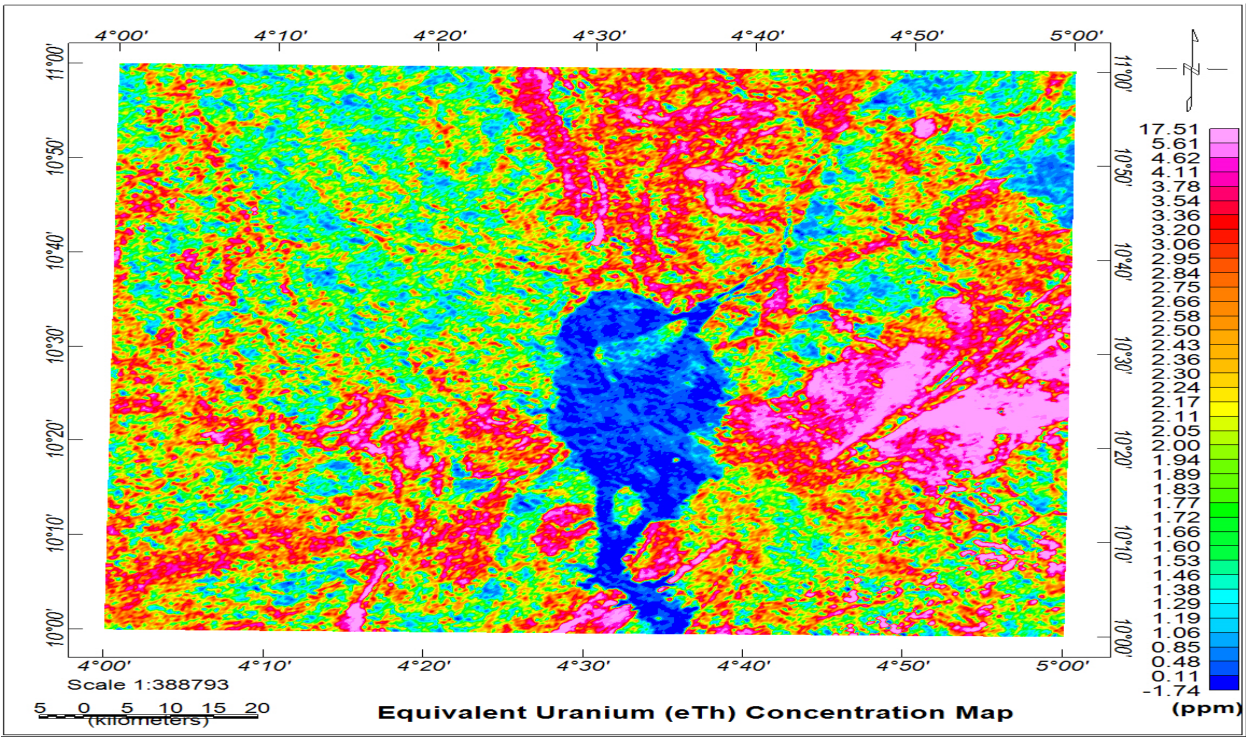


**Fig. 9c Equivalent Uranium (eU ppm) Concentration Map**

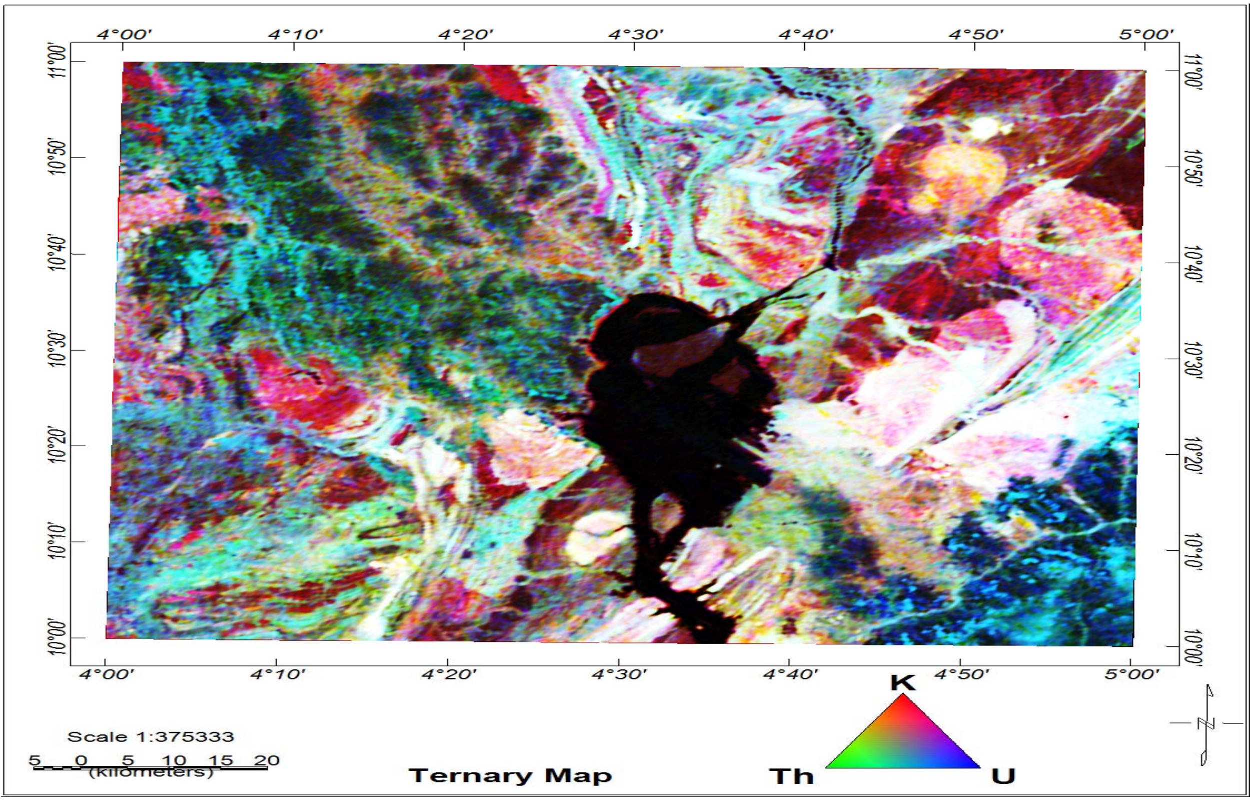


**Fig. 10 Ternary Map the Study Area**

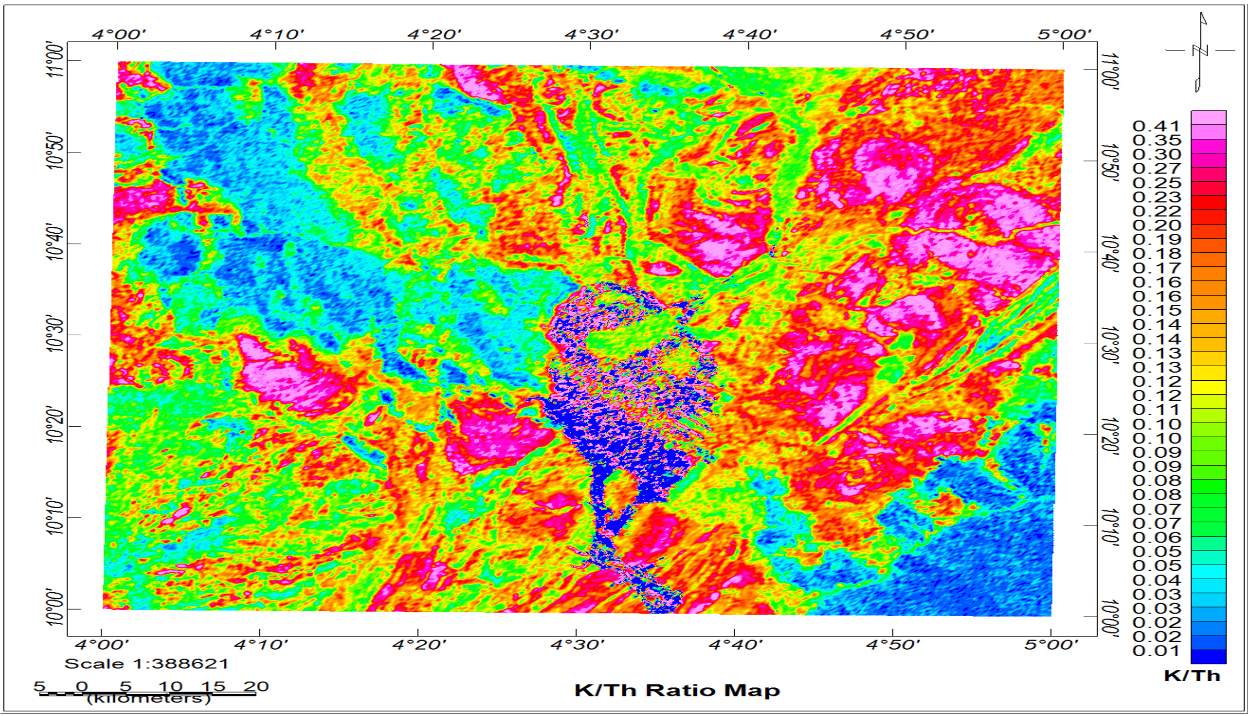


**Fig. 10 Potassium-Equivalent Thorium Ratio (K/eTh) Map**

## V. Conclusion

Airborne magnetic data obtained for upper Sokoto and lower Bida Basin ware analyzed by employing several enhancement techniques to mapped the lithology, geological structures, lineament orientation, and hydrothermal alteration associated with possible gold mineralization potential zones in the study area.

The results obtained from first and second vertical derivatives reveals two major formations the positive anomalies coincide with prevalent sedimentary and the negative anomalies is associated with crystalline basement complex, the analytical signal map also reveal the area of basement complex and sedimentary basin, the CET lineament analysis map (fig. 6) show that the lineaments orientation trending NNE-SSW direction, densely and predominantly NE-SW of the study area. The vast presence of lineaments suggests that the existence of fault, fractures, vain and dykes etc. In the CET porphyry analysis of geologic contact map (fig. 7) shows depicts within the basements and dike-like features are more abundant above the crystalline basement and may be the areas of mineralization potential because menials are structurally control. Similarly, the depth to magnetic source was determined using SPI and ranges 68.21m to 229.68m for shallow basement and 305.73m to 2979.17m for deep magnetic source.

The aeroradiometric maps generated helped in mapping the geologic structures, areas of high concentration, law and moderate radiation signatures. The composite image technique applied to radiometric data allows the identification and delineation of lithological units based on slight variations in concentrations of radioelements. The potassium Thorium ratio map of the study area successfully identified zones with significant range of hydrothermal alteration values 0.18 to 0.41 K / eTh ratio, Hoover *et al.,* 1992) stated that areas with remarkable values outside 0.17 to 0.2 (K/Th in%/ppm the area affected is zones of high gold mineralization potentials

## References

[1] Adekeye, J. I. D., Ajadi, J., Adedoyin, A. D., Bamigboye, O. S., &Alabi, A. G. F. (2015). Origin and Structural Control of Gold

[2] Mineralization in Bishewa Area, Central Nigeria. CPJ, 2015002, 211012.

[3] Adepelumi, A. A., & Falade, A. H. (2017). Combined high-resolution aeromagnetic and radiometric mapping of uranium mineralization and tectonic settings in Northeastern Nigeria. Acta Geophysica, 65(5), 1043-1068.

[4] Adewumi, T., & Salako, K. A. (2018). Delineation of mineral potential zone using high resolution aeromagnetic data over part of Nasarawa State, North Central, Nigeria. Egyptian journal of petroleum, 27(4), 759-767.

[5] Ajibade, A.C. and Wright, J.B. (1989). The Togo-Benin-Nigeria shield: evidence of crustal aggregation in the Pan-African belt. Tectonophys 165, pp. 125-12.

[6] Ajibade, A.C., Woakes, M. and Rahaman, M.A. (1987). Proterozoic crustal development in the Pan-African regime of Nigeria. In A.

[7] Krooner (Editor), Proterozoic Crustal Evolution. Geodynamics. Ser., Am. Geophysics Union, 17: pp259-271.

[8] Armstrong M, Rodeghiero A (2006). Airborne Geophysical Techniques in Aziz. Coal Operators' Conference, University of Wollongong and the Australasian Institute of Mining and Metallurgy pp. 113-131. Briggs IC (1974). Machine contouring using minimum curvature. Geophysics 39(1):39-48.

[9] Ajibade, A.C., Woakes, M. and Rahaman, M.A. (1987). Proterozoic crustal development in the Pan-African regime of Nigeria. In: A. Krooner (Editor), Proterozoic Crustal Evolution. Geodynamics. Ser., Am. Geophysics Union, 17: pp259-271.

[10] Akande, S. O., & Kinnaird, J. (1993). Characterization and origin pf ore-forming fluids in the Nigeria mineral belts. In Quadrennial IAGOD symposium (pp. 199-218).

[11] Amigun, J. O., Afolabi, O., & Ako, B. D. (2012). Application of airborne magnetic datato mineral exploration in the Okene Iron Ore Province of Nigeria. International Research Journal of Geology and Mining, 2(6), 132-14.

[12] Biegert, E. K., Chapin, D. A., Yalamanchili, S. V., Daggett, P. H., Pearson, W. C., Bird, D. E., ... & Nakatsuka, T. (1998). Basin Studies. In Geologic Applications of Gravity and Magnetics: Case Histories (pp. 45-72). Society of Exploration Geophysicists and American Association of Petroleum Geologists.

[13] Chukwuka, C. (2016). Integrated Landsat ETM and Aeromagnetic Survey for enhanced structural and geothermal interpretation of part of Calabar Flank. Unpubl. Thesis, 113p.

[14] Collins R (2005) Aeromagnetic surveys principles, practice and interpretations. Geosoft, Netherlands.

[15] FEEBREY, C. A., HISHIDA, H., YOSHIOKA, K., & NAKAYAMA, K. (1998).

[16] Geophysical Expression of Low Sulphidation Epithermal Au-Ag Deposits and Exploration Implications–Examples from the Hokusatsu Region of SW Kyushu, Japan–. Resource Geology, 48(2), 75-86.

[17] Dentith M, Mudge ST (2014) Geophysics for the mineral exploration geoscientist. Cambridge Univesity Press, Cambridge. ISBN

[18] 978-0-521-80951.

[19] Garba, (1994). Tourmalinization related to Late-Proterozoic-Early Paleozoic Lode Gold Mineralization in Birnin Yauri Area, Nigeria, Mineralium Deposita 31(1994):201.

[20] Gupta, V. H., & Ramani, S. D. (1982). Optimum Second Vertical Derivative Application in Geological Mapping and Mineral Exploration. Geophysics, 24, 582-601.

[21] Hinze, W. J., Von Frese, R. R., & Saad, A. H. (2013). Gravity and magnetic exploration: Principles, practices, and applications. Cambridge University Press.

[22] Holden, E. J., Dentith, M., & Kovesi, P. (2008). Towards the automated analysis of regional aeromagnetic data to identify regions prospective for gold deposits. Computers & Geosciences, 34(11), 1505-1513.

[23] Holden, E. J., Fu, S. C., Kovesi, P., Dentith, M., Bourne, B. and Hope, M., 2011. Automatic Identification of Responses from Porphyry Intrusive Systems within Magnetic Data Using Image Analysis. Journal of Applied Geophysics, Vol. 74, pp. 255 - 262.

[24] Hoover, D. B., Heran, W. D., & Hill, P. L. (1992). The geophysical expression of selected mineral deposit models. US Department of the Interior, Geological Survey.

[25] Irvine, R. J., & Smith, M. J. (1990). Geophysical exploration for epithermal gold deposits. Journal of Geochemical exploration, 36(1-3), 375-412.

[26] Keating, P. and Sailhac, P. (2004). Use of the Analytical Signal to Identify Magnetic Anomalies due to Kimberlite Pipes. Geophysics 69(1):180-190.

[27] Kovesi, P., 1991. Image Features from Phase Congruency. Videre: Journal of Computer Vision Research, the MIT Press, Vol. 1, No. 3.

[28] Kovesi, P., 1997. Symmetry and Asymmetry from Local Phase.AI'97, Tenth Australian Joint Conference on Artificial Intelligence.

[29] Lam, L., Lee, S. W. and Suen, C. Y., 1992. Thinning Methodologies—A Comprehensive Survey. IEEE Transactions on Pattern Analysis and Machine Intelligence, Vol. 14, No. 9, pp. 879.

[30] Macnae, J. (1995). Applications of geophysics for the detection and exploration of kimberlites and lamproites. Journal of Geochemical Exploration, 53(1-3), 213-243.

[31] McCurry, P. (1978). Geology of degree sheets 19 (Zuru), 20 (Chafe), and part of 19 (Katsina), Nigeria, Overseas Geological Mineral Resource., 53p.

[32] Morrell, A. E., Locke, C. A., Cassidy, J., & Mauk, J. L. (2011). Geophysical characteristics of adularia-sericite epithermal gold-silver deposits in the Waihi-Waitekauri region, New Zealand. Economic Geology, 106(6), 1031-1041.

[33] Obaje, N. G. (2009). Geology and mineral resources of Nigeria (Vol. 120). Springer.

[34] Opara, A. I., Oneyekuru, S. O., Mbagwu, E. C., Emberga, T. T.,

[35] Ijeomah, K. C. & Nwokocha, K. C. (2015). Integrating Landsat – ETM and Aeromagnetic Data for Enhanced Structural Interpretation over Naraguta Area, North-Central Nigeria. International J. of Scientific and Engineering Research, 6(9), 10 .

[36] Opara, A. I., Onyewuchi, R. A., Selemo, A. O. I., Onyekuru, S. O., Ubechu, B. O., Emberga, T. T., Ibim, D. F., & Nosiri, O. P. (2014). Structural and Tectonic Features of Ugep and Environs, Calabar Flank, Southeastern Nigeria: Evidences from aeromagnetic and Landsat-ETM data. Mittei lungenKlosterneuburg, 64, 22.

[37] Osinowo, O. O., Akanji, A. O., & Olayinka, A. I. (2014). Application of high-resolution aeromagnetic data for basement topography mapping of Siluko and environs, southwestern Nigeria. Journal of African Earth Sciences, 99, 637-651.

[38] Ostrovskiy, E.A. (1975) Antagonism of Radioactive Elements in Well Rock Alteration Fields and Its Use in Aerogamma Spectrometric Prospecting. International Geological Review, 17, 461-468.

[39] Power, M., Belcourt, G., & Rockel, E. (2004). Geophysical methods for kimberlite exploration in northern Canada. The Leading Edge, 23(11), 1124-1129.

[40] Reeves, C. (2005). Aeromagnetic surveys: principles, practice and interpretation (Vol. 155). Toronto: Geosoft.

[41] Roest, W.R, Verhoef, J., and Pilkington, M. (1992). Magnetic interpretation using the 3-D analytical Signal. Geophysics 57(6):116-125.

[42] Roux, A. (1967). The Application of Geophysics to Gold Exploration in South Africa 425-438.

[43] Salako, K. A. (2014). Depth to basement determination using Source Parameter Imaging (SPI) of aeromagnetic data: An application to upper Benue Trough and Borno Basin, Northeast, Nigeria. Academic Research International, 5(3), 74.

[44] Silva, A.M., Pires, A.C.B., Mccafferty, A., de Moraes, R.A.V. and Xia, H. (2003) Application of Airborne Geophysical Data to Mineral Exploration in the Uneven Exposed Terrains of the Rio Das Velhas Greenstone Belt. Revista Brasileira de Geociências, 33, 17-28.

[45] Core D, Buckingham A, Belfield S. Detailed structural analysis of magnetic data done quickly and objectively, SGEG Newsletter; 2009.

[46] Wemegah, D. D., Preko, K., Noye, R. M., Boadi, B., Menyeh, A., Danuor, S. K., & Amenyoh, T. (2015). Geophysical interpretation of possible gold mineralization zones in Kyerano, south-western Ghana using aeromagnetic and radiometric datasets.